

Colliding Stellar Wind Models with Nonequilibrium Ionization: X-rays from WR 147

Svetozar A. Zhekov*

Space Research Institute, Sofia-1000, Moskovska str. 6, Bulgaria

ABSTRACT

The effects of nonequilibrium ionization are explicitly taken into account in a numerical model which describes colliding stellar winds (CSW) in massive binary systems. This new model is used to analyze the most recent X-ray spectra of the WR+OB binary system WR 147. The basic result is that it can adequately reproduce the observed X-ray emission (spectral shape, observed flux) but some adjustment in the stellar wind parameters is required. Namely, (i) the stellar wind velocities must be higher by a factor of 1.4 – 1.6; (ii) the mass loss must be reduced by a factor of ~ 2 . The reduction factor for the mass loss is well within the uncertainties for this parameter in massive stars, but given the fact that the orbital parameters (e.g., inclination angle and eccentricity) are not well constrained for WR 147, even smaller corrections to the mass loss might be sufficient. Only CSW models with nonequilibrium ionization and equal (or nearly equal) electron and ion postshock temperature are successful. Therefore, the analysis of the X-ray spectra of WR 147 provides evidence that the CSW shocks in this object must be *collisionless*.

Key words: stars: individual: WR 147 - stars: Wolf-Rayet - X-rays: stars - shock waves

1 INTRODUCTION

The Wolf-Rayet (WR) star WR 147 (AS 431) is a classical example of colliding stellar wind (CSW) binary: it possesses relatively strong X-ray emission and it is a nonthermal radio source. Probably the most interesting piece of information about this WR+OB binary system comes from the radio, namely, high-resolution interferometer observations have spatially resolved its emission into two components: a southern thermal source, WR 147S (the WN 8 component in the binary), and a northern nonthermal source, WR 147N (Abbott et al. 1986; Moran et al. 1989; Churchwell et al. 1992; Contreras et al. 1996; Williams et al. 1997; Skinner et al. 1999, hereafter S99). Moreover, long-term radio variability has been reported both from the thermal (Contreras & Rodriguez 1999) and nonthermal (Setia Gunawan et al. 2001) sources. The radio spectrum of WR 147S has a spectral index $\alpha = +0.6; +0.62$ ($S_\nu \propto \nu^\alpha$), which is very close to the canonical value for the thermal free-free emission from ionized stellar winds (Churchwell et al. 1992; Williams et al. 1997; S99). On the other hand, the nonthermal radio emission of WR 147N cannot be described by a simple power law, which is expected from synchrotron models that assume power-law electron energy distribution (S99), and more elaborated

modelling is required (Dougherty et al. 2003; Pittard et al. 2006).

High-resolution infrared images clearly showed the NIR counterparts of the two radio sources located at $\approx 0''.64$ from each other and WR 147N was classified as a B0.5V star (Williams et al. 1997) but an earlier spectral class, O8-O9 V-III, was suggested from the *Hubble Space Telescope* observations (Niemela et al. 1998). Given the distance to WR 147 of 630 ± 70 pc (Churchwell et al. 1992), the projected (or minimum) binary separation is 403 ± 13 au. It is worth noting that analyzing radio and IR images, Williams et al. (1997) have found that the WR 147N radio peak is displaced by $0''.07$ southward from its IR counterpart. Although this value is within the uncertainties of the data, if it is real, then the nonthermal radio source can be associated with the CSW region located off the surface of the OB companion. This physical picture found further support from the high spatial resolution *Chandra* image, showing that the X-ray emission peak lies at or near WR 147N (Pittard et al. 2002).

The X-ray observations of WR 147 have revealed the presence of thermal emission from high temperature plasma but they also demonstrated how it is important to have data with good quality. Namely, WR 147 was first detected by the *Einstein* observatory and it was concluded that the X-rays are due to plasma at temperature $kT \geq 0.5$ keV (Caillault et al. 1985). Analysis of the moderate resolution CCD spectra, ob-

* E-mail: szhekov@space.bas.bg

tained with *ASCA* and having not very high photon statistics, suggested that the X-rays likely originate in multitemperature plasma whose cooler component has a temperature of $kT \approx 1$ keV, but the characteristics of the hotter component could not be constrained (S99). Finally, the higher signal-to-noise *XMM-Newton* data of WR 147 presented by Skinner et al. (2007, hereafter S07) have undoubtedly revealed the elusive high temperature plasma in this object by detecting the Fe $K\alpha$ complex at 6.67 keV. The corresponding analysis of the X-ray spectra has shown that the plasma temperature is as high as $kT = 2.7$ keV. The authors pointed out that neither long-term X-ray variability nor changes in the X-ray absorption were detected. Thus, the ‘evolution’ of the plasma characteristics, mentioned above, is merely a result of the acquisition of higher quality data with each successive generation of X-ray satellites.

Apart from the clear evidence for presence of high temperature plasma in WR 147, S07 have found indications that further improvement of numerical CSW models is needed. Namely, higher terminal wind velocities are required to account for the hot plasma detected in this object, and future CSW models must include some additional physics such as nonequilibrium ionization (NEI).

Motivated by this, the aim of this study was to develop new CSW models that take into account the NEI effects and then to confront them with the high quality *XMM-Newton* spectra of WR 147. The model details are given in § 3. The results from the model application are presented in § 4 and discussed in § 5. Our conclusions are found in § 6.

2 DATA

The X-ray observations of WR 147 were performed with the *XMM-Newton* observatory in November 2005. All the details about the EPIC data and the data reduction are found in S07. We only note that our analysis is based on the PN and MOS spectra of WR 147 and the latter is the sum of the spectra from the two MOS detectors. Thus, each analyzed spectrum has about the same number of counts (4436 in PN; 4148 in combined MOS). They were rebinned to have a minimum of 20 cts per bin. All spectral fits were performed in the recent version (11.3.2) of the software package for analysis of X-ray spectra, XSPEC (Arnaud 1996). The spectra were analyzed simultaneously with exactly the same model and only the XSPEC normalization parameter was decoupled to allow for any calibration difference between the PN and MOS detectors.

3 MODEL

The goal of this study is to use a realistic model that determines the physical parameters of the X-ray emitting plasma, and on its basis to simulate the X-ray spectra to be confronted with the observational data. A good starting point is to consider a simple model which describes the basic physical situation and then elaborate on those that include more complex physics (e.g., nonuniform gas flows, thermal conduction etc.) which might be potentially important for the case under consideration. As in the case of other wide stellar

binaries (e.g., WR 140; Zhekov & Skinner 2000), an adiabatic model of CSW interaction was adopted for describing this phenomenon in WR 147 while more complicated models are beyond the scope of the present work. Adiabatic CSWs also have the advantage that the hydrodynamic solution in the interaction region does not depend on such details as: e.g., exact metal abundances, whether or not the plasma is in ionization equilibrium, or any difference between electron and ion temperatures. On the other hand, any of these may directly affect the shape of the emitted X-ray spectrum and the strength of various emission lines. Thus, it might be necessary to take them into account when simulating the X-ray emission from such objects. We note that all these physical characteristics allow the X-ray spectral simulations to be decoupled from the hydrodynamic modelling of CSWs in wide binaries. Namely, the temperature and density distributions of the hot plasma, as initially derived from the numerical hydrodynamics, can be further postprocessed to model the corresponding X-ray emission. We next describe the steps in such an approach as applied to the case of WR 147.

3.1 CSW Model

A primary step is to determine the distribution of temperature and density of the X-ray emitting plasma. For this purpose, the hydrodynamic model of adiabatic CSWs by Myasnikov & Zhekov (1993, hereafter MZh93) was used to derive the physical parameters in the interaction region of WR 147. This model assumes spherical symmetry of the supersonic stellar winds that have attained their terminal velocities in front of the shocks. This assumption is well justified for wide stellar binaries where neither the radiative braking nor the orbital motion is expected to play an important role for the wind dynamics. In this case, the interaction region has cylindrical symmetry and the gasdynamic problem is determined entirely by the stellar wind parameters and the binary separation. We note that the ‘shock fitting’ technique is used in this numerical model, and thanks to this an exact solution to all discontinuity surfaces (the two shocks and the contact discontinuity) is derived. This means that there is no numerical ‘mixing’ between the shocked gases of the stellar winds which further facilitates modelling the X-ray emission from the hot plasma, especially, when the different chemical composition is concerned. The procedure of how the effects of different electron and ion temperatures can be taken into account is described in Zhekov & Skinner (2000) and that for handling the nonequilibrium ionization is given below.

3.2 NEI Effects

In many astrophysical examples, the plasma emission is determined by the state of ionization equilibrium. If plasma characteristics such as temperature and density evolve on relatively small timescales, some time is also needed for a new state of ionization equilibrium to be established. Therefore, we might have a chance to witness transition phases in the plasma evolution. One such case is when the astrophysical plasmas are heated by shocks: gas temperature and density experience abrupt change. Fast shocks, as in supernova remnants or CSW binaries, can result in high plasma temperatures, and the corresponding hot-plasma emission is

entirely determined by the collisional processes of ionization and excitation mostly with electrons. A detailed description of related processes that determine the hot-plasma emission both in and out of ionization equilibrium can be found in the review papers by Liedahl (1999) and Mewe (1999).

Obviously, the transition phases, such as the state of nonequilibrium ionization, are important in evolving systems. On the other hand, the NEI effects might play an important role also in steady state conditions as in the CSW shocks in wide binaries. Namely, despite the fact that the general picture does not change in time, each individual parcel of gas follows the same ‘evolutionary’ pattern: it gets heated on the shock front, and then its ionization state relaxes downstream towards the corresponding equilibrium conditions: collisional ionization equilibrium (CIE). Whether or not the transition phase is important depends on how quickly CIE is established with respect to the typical timescale of the flow.

In order to determine the relative importance of the NEI effects in CSW binaries, we consider a dimensionless parameter $\Gamma_{nei} = \tau/\tau_{nei}$. Here τ is the timescale of gasdynamics and τ_{nei} is the characteristic time to establish ionization equilibrium, which we can refer to as the NEI timescale. The NEI effects must be taken into account if $\Gamma_{nei} \leq 1$ but can be neglected for $\Gamma_{nei} \gg 1$. In the hydrodynamic model at hand, $\tau = D/V_\infty$, where $2D = a$ is the separation between the binary components and V_∞ is the terminal stellar wind velocity. Unfortunately, there is no ‘unique’ NEI timescale and such a parameter can be introduced for each chemical element whose ionization state is considered. Although the latter requires one to solve a set of differential equations, qualitative considerations show that CIE is controlled mostly by the rate coefficients of collisional ionization and recombination to hydrogen- and helium-like species of a given chemical element. This is particularly the case for hot, X-ray emitting plasmas that are of interest in this study. Guided by this (see also the NEI discussion and the case example of oxygen in Liedahl 1999), we can introduce a representative NEI timescale $\tau_{nei} = 10^{12}/n_e$, where n_e is the electron number density of the hot plasma. In that case Γ_{nei} can be expressed in terms of the basic CSW parameters:

$$\Gamma_{nei} = 1.21 \frac{\chi_e \dot{M}_5}{\bar{\mu} V_{1000}^2 D_{16}} \quad (1)$$

where \dot{M}_5 is the mass-loss rate in units of $10^{-5} M_\odot \text{ yr}^{-1}$, V_{1000} is the stellar wind velocity in units of 1000 km s^{-1} , $D_{16} = D/10^{16} \text{ cm}$, $\bar{\mu}$ is the mean atomic weight for nucleons, and $\chi_e = n_e/n$ is the relative electron number density (n is the nucleon number density).

Given the stellar wind and binary parameters of WR 147 (see § 3.4), it is anticipated that the NEI dimensionless parameter $\Gamma_{nei} \approx 1$ and $\Gamma_{nei} \ll 1$ for the shocked WR and O wind, respectively. This means that the NEI effects likely play an important role for the X-ray emission from the CSW region in this object.

Keeping in mind the cylindrical symmetry of the hydrodynamic problem, a full set of 2D, time-dependent partial differential equations must be considered if the NEI effects need be taken into account in the CSW models. From a numerical view point, an alternative to this is to consider the ionization balance along the flow streamlines. In this case the numerical task is much simpler and a set of ordinary

differential equations represents the evolution of the ionization state of each chemical element:

$$\frac{dn_i}{d\tau_e} = C_{i-1}n_{i-1} - (C_i + \alpha_i)n_i + \alpha_{i+1}n_{i+1} \quad (2)$$

where C and α denote the collisional ionization and recombination rate coefficients, respectively, and $n_{i-1,i,i+1}$ are the number densities of any three consecutive ionization stages of a given chemical element. The parameter τ_e is the so-called ionization time, $\tau_e = \int n_e dt$, and the integration starts at the shock front and is carried out downstream along a specific streamline.

It is well known that the ionization equations (eqs. [2]) are a set of *stiff* ordinary differential equations, and various techniques have been developed to deal with this numerical problem. Very often an eigenfunction method (e.g. Hughes & Helfand 1985) is used to solve these equations efficiently, and this method was adopted in various NEI models available in XSPEC (Borkowski, Lyerly & Reynolds 2001). Therefore, the latter was the basis for incorporating our NEI CSW models in the spectral fits to the X-ray data of WR 147. We note that the NEI models in XSPEC usually assume constant electron density and temperature while this is not the case in the density and temperature stratified interaction region in CSW binaries. To overcome this problem, we adopted a piecewise integration approach. Namely, the hydrodynamic model allows for deriving all the necessary plasma parameters (e.g., number density, electron temperature, ionization time) at the grid points along a given streamline of the flow. It is thus assumed that density and temperature are constant in between any two consecutive (j and $j+1$) grid points along the streamline and now the NEI problem can be solved using the corresponding models available in XSPEC (with the only modification that at each step the initial values for eqs. [2] are those from the previous grid point). Once this is done, the X-ray spectrum of the hot plasma along a given streamline is derived and the sum over all the streamlines gives the total X-ray emission from the interaction region.

3.3 CSW Models in XSPEC

In order to make a direct comparison between the observations and the X-ray emission predicted by the CSW models, we developed a new spectral model for XSPEC. The X-ray emission from the interaction region is thermal, thus, its characteristics are determined by the temperature, emission measure and chemical abundances of the hot plasma. This is true for the case of CIE and an additional parameter (ionization time) should be provided as well, if the NEI effects are important. All these necessary ingredients are given by the hydrodynamic CSW model. For modelling the X-ray emission in CIE the XSPEC optically-thin plasma model *apec* is used at each grid point of the interaction region, while the case of NEI is considered as described above (§ 3.2). Such an approach also has the advantage that the fits with theoretical spectra of CSW binaries can be easily confronted with the results from the standard fits that usually make use of discrete-temperature plasma models (both in and out of ionization equilibrium) available in XSPEC (e.g., *vmekal*, *vapex*, *vpshock*). This, in turn, will be helpful for interpreting the X-ray data from CSW binaries when detailed numeri-

cal modelling is not feasible for various reasons (e.g., data quality, binary parameters are not available).

Two types of test were performed for the new spectral models. First, for internal consistency, the distribution of emission measure of the hot plasma, as derived on the original grid of the hydrodynamic CSW model, was compared with the one resulting from the integration along the flow streamlines. Second, results from our piecewise integration approach were confronted with the ones from the XSPEC *vpshock* model. These tests made us confident about the further use of the spectral CSW models for analyzing the *XMM-Newton* data of WR 147.

Finally, using the known distance to the observed object, the emission measure from the hydrodynamic CSW model can be converted into XSPEC units¹. In such a case, the XSPEC *norm* parameter of our spectral model would have values close to unity if theoretical and observed fluxes match each other. Deviations from unity may be an indication of inaccuracies in the adopted stellar wind parameters or the distance to the object.

3.4 Basic Parameters for the CSW Model in WR 147

For consistency with previous works (S99, S07), we define a ‘standard’ CSW model for WR 147, which will also serve as a starting point for the fits to the X-ray emission from this object. As already mentioned, the distance of 630 pc to WR 147 is adopted in this study, and the stellar wind parameters are: $\dot{M}(WR) = 4 \times 10^{-5} M_{\odot} \text{ yr}^{-1}$, $v_{\infty}(WR) = 950 \text{ km s}^{-1}$, $\dot{M}(O) = 6.6 \times 10^{-6} M_{\odot} \text{ yr}^{-1}$, $v_{\infty}(O) = 1600 \text{ km s}^{-1}$. These values define a wind momentum ratio $\eta = [\dot{M}(O)v_{\infty}(O)]/[\dot{M}(WR)v_{\infty}(WR)] = 0.028$ (note that $\Lambda = 1/\eta$ is used in MZh93 for the wind momentum ratio, but for consistency with the work of other authors η will be used throughout this study). Also, a minimum value of the stellar separation in this binary system is $a = 2D = 403 \text{ au}$, and we note that this parameter depends on the inclination angle which is uncertain. Based on analysis of VLA radio images, values of $i = 45^{\circ} \pm 15^{\circ}$ (Contreras & Rodriguez 1999) and $i \approx 30^{\circ}$ (Contreras, Montes & Wilkin 2004) have been reported but other values may well be possible. It is so since the inclination angle was derived by fitting a thin shell model to the radio image and it should be kept in mind that such a model can not be considered satisfactory for wide stellar binaries, where the CSWs are adiabatic, since it gives only the shape of the contact discontinuity surface. On the other hand, the shape of the shock surfaces (e.g., their ‘opening angle’) is quite different which makes results from such a model application highly uncertain. Therefore, values for the binary separation in WR 147 a few times larger than the minimum value given above are not ruled out.

Thus, we have all the necessary input parameters for the hydrodynamic CSW model at hand (MZh93), and elemental abundances have to be provided for modelling the thermal

X-ray emission from the interaction region. Due to their advanced evolutionary status, WR stars are objects with non-solar abundances and for this study the following set of them is adopted. The abundances for H, He, Ne and Ca are based on the analysis of the IR spectrum of WR 147 (Morris et al. 2000), and the other elements have values ‘typical’ for a WN star (van der Hucht, Cassinelli & Williams 1986). For convenience, all values are with respect to the solar number abundances (unity means solar abundance as in Anders & Grevesse 1989): H = 1, He = 25.6, C = 0.9, N = 140, O = 0.9, Ne = 44.3, Mg = 14.4, Si = 15.2, S = 3.6, Ar = 5, Ca = 4.7, Fe = 7, Ni = 1 (no information is available for Ni and it was assumed solar but we note that the spectral fits are not sensitive to its value). Due to the high X-ray absorption, the portion of the spectrum with good statistics ($E \geq 0.9 \text{ keV}$) is sensitive only to the elemental abundances of Ne, Mg, Si, S, Ar, Ca, Fe, which are allowed to vary in our fits. In all fits the elemental abundances of the O wind were strictly solar and they are kept fixed in the modelling of the X-ray emission from WR 147. The assumed WN abundances correspond to a relative electron density $\chi_e = 1.71$, mean particle weight (electrons and nucleons) $\mu = 1.16$, and mean atomic weight for nucleons $\bar{\mu} = 3.14$. For the O star the adopted abundances give $\chi_e = 1.1$, $\mu = 0.62$ and $\bar{\mu} = 1.3$.

4 RESULTS

The results from previous application of the hydrodynamic CSW model for calculating the X-ray emission from WR 147 indicated that there is a luminosity mismatch between the model predictions and the observations (S99, S07). Namely, the theoretical luminosity (or the amount, emission measure, of the hot plasma) is $\sim 3 - 4$ times larger than observed. Our new spectral analysis confirmed that this difference between theory and observations is now valid for both cases of CIE and NEI, if the *nominal* wind parameters are used (e.g., the ones defined in § 3.4). This conclusion also holds if the mass loss of the O star, $\dot{M}(O)$, is varied. Two such cases were considered which have $\eta = 0.02$ ($\dot{M}(O) = 4.7 \times 10^{-6} M_{\odot} \text{ yr}^{-1}$) and 0.04 ($\dot{M}(O) = 9.4 \times 10^{-6} M_{\odot} \text{ yr}^{-1}$), respectively (note that all other parameters, $\dot{M}(WR)$, $v_{\infty}(WR)$, $v_{\infty}(O)$, kept their *nominal* values, § 3.4). Moreover, in all the three cases, $\eta = 0.02, 0.028$ and 0.04 , the overall quality of the fits is not acceptable as indicated by the values of reduced $\chi_{\nu}^2 = 1.63 - 1.93$ (with degrees of freedom $\nu = 332$ for all the fits considered throughout this study). Therefore, it is conclusive that the CSW model not only predicts an amount of X-rays larger than that observed for WR 147, but it also does not give a good match to the exact shape of the observed X-ray spectrum, especially, in its high-energy part above 4 keV, where the theoretical spectrum is softer than the observed one. Obviously, the data require presence of a hotter plasma in the interaction region and, as already suggested, a remedy to this problem could be the assumption of higher values for the stellar wind velocities (S07). Note that the contribution of the shocked O wind is no more than 12-15% at energies above 4 keV (S07 and this work), therefore, the velocity of the WN wind is a crucial parameter.

To explore this possibility, a set of CSW models (both in CIE and NEI) was considered with increased wind velocities

¹ Conversion of emission measure into XSPEC units is done by multiplying it with the term $10^{-14}/4\pi d^2$, where d is the distance to the object in cm. This term comes from the XSPEC normalization factor of the flux for optically-thin plasma models.

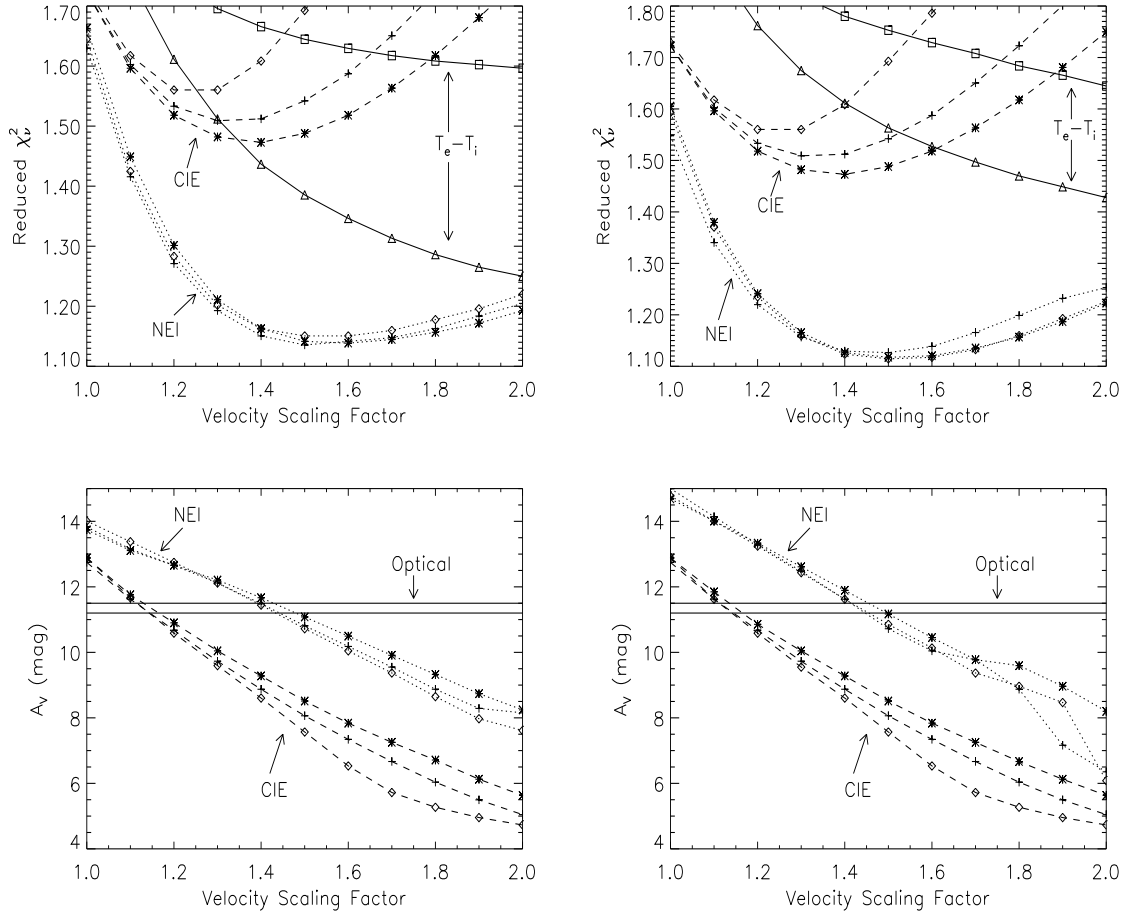


Figure 1. Results from the CSW model fits. **Left column:** Mass-loss rates scaled while the binary separation is kept at its ‘nominal’ value. **Right column:** The binary separation is scaled while mass-loss rates have their ‘standard’ values. **Upper panels:** Reduced χ^2_ν vs. scaling factor for the wind velocities. Dotted lines denote the models with nonequilibrium ionization (NEI), and dashed lines present models that assume the hot plasma is in collisional ionization equilibrium (CIE). The plus signs are for the case of $\eta = 0.04$; asterisks mark models with $\eta = 0.028$; and diamonds present models with $\eta = 0.02$. The solid lines illustrate the effect of nonequilibrium electron and ion temperatures ($\beta = T_e/T_i = 0.2$) for $\eta = 0.028$ as triangles are for models with NEI while squares present those in CIE. **Lower panels:** The visual extinction as derived from the fits with various models where the N_H to A_V conversion formula from Gorenstein (1975) was used. All symbols and lines have the same meaning. The two horizontal solid lines give the optical extinction deduced from IR studies ($A_V = 11.5$ mag, Churchwell et al. 1992; $A_V = 11.2$ mag, Morris et al. 2000). The degrees of freedom in all the fits are $\nu = 332$.

for all the three basic cases ($\eta = 0.02, 0.028$ and 0.04). It is anticipated that increasing wind velocities will make the NEI effects more pronounced (see eq. [1]).

On the other hand, assuming the distance to WR 147 is well constrained (630 ± 70 pc, Churchwell et al. 1992) the mass loss or the binary separation should be changed in order to solve the problem with the luminosity (emission measure) mismatch. Namely, it is necessary to decrease the emission measure in the interaction region which can be done in two ways: (i) by decreasing the mass loss rates; (ii) by increasing the binary separation. This follows from the relation between the emission measure in the interaction region and the parameters for spherically symmetric stellar winds:

$$EM = \int n_e n_H dV \propto \frac{\dot{M}^2}{v_{wind}^2 D^2}$$

where $n_e, n_H \propto \frac{\dot{M}}{v_{wind} D^2}$, and $V \propto D^3$. As we see, increasing the wind velocity also means a smaller value for the emission

measure, but we note that the general effect of this quantity is to control the shape of the resultant X-ray spectrum since the wind velocities are directly related to the plasma temperature in the interaction region.

Thus, to discriminate between influences of various CSW parameters on the X-ray emission from WR 147, the basic cases mentioned above, $\eta = 0.02, 0.028$ and 0.04 , were considered in two different ways. First, the mass loss rates of the both stellar winds were scaled simultaneously by a factor of 0.6 ($\eta = 0.02$), 0.5 ($\eta = 0.028$), and 0.4 ($\eta = 0.04$), while the binary separation had its ‘standard’ value. Second, the mass losses kept their nominal values while the binary separation was increased correspondingly by a factor of 3 ($\eta = 0.02$), 4 ($\eta = 0.028$), and 6.25 ($\eta = 0.04$). For each of the three basic cases, a grid of model fits was performed as the wind velocities changed with the same scaling factor that varied between 1 and 2. Adopting such an approach, namely, to scale the mass losses and/or the wind velocities

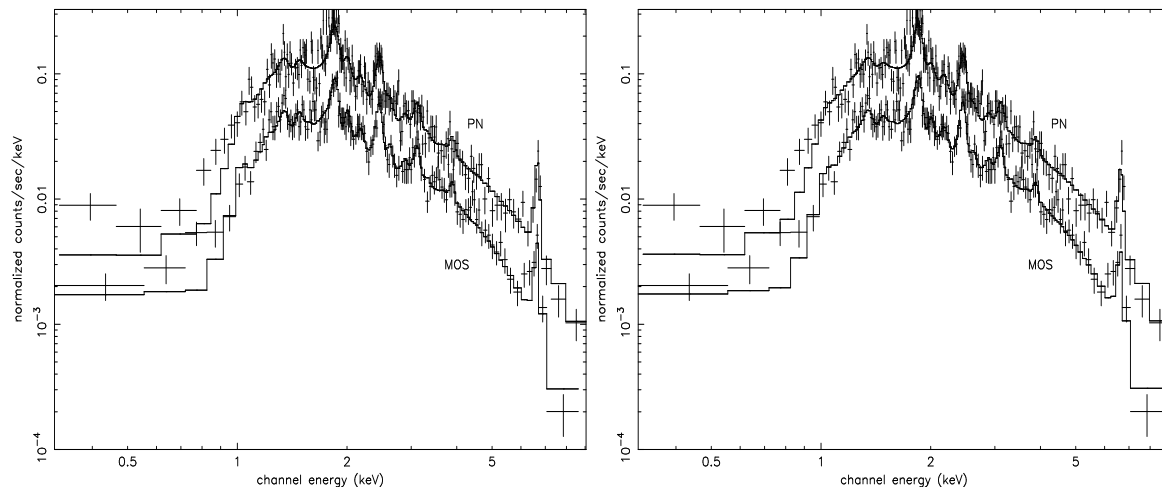


Figure 2. Examples of background-subtracted PN and MOS (MOS1+MOS2) spectra of WR 147 and the corresponding best fit NEI CSW models for $\eta = 0.028$ and stellar wind velocities scaled by a factor of 1.5. **Left panel:** the case of reduced mass losses by a factor of 0.5. **Right panel:** the case with increased binary separation by a factor of 4. Fit results are given in Table 1.

Table 1. Examples of CSW ($\eta = 0.028$) spectral fits for WR 147

| | Mass loss ^(a) | Binary separation ^(b) |
|--------------------------------|--------------------------|----------------------------------|
| χ^2/dof | 379/332 | 371/332 |
| $N_H(10^{22} \text{ cm}^{-2})$ | 2.46 [2.30 - 2.64] | 2.48 [2.32 - 2.64] |
| H | 1 | 1 |
| He | 25.6 | 25.6 |
| C | 0.9 | 0.9 |
| N | 140.0 | 140.0 |
| O | 0.9 | 0.9 |
| Ne | 16.9 [7.1 - 32.6] | 5.8 [0.3 - 13.7] |
| Mg | 3.5 [1.9 - 5.9] | 1.6 [0.5 - 2.9] |
| Si | 5.1 [4.1 - 6.3] | 3.7 [3.1 - 4.5] |
| S | 7.8 [6.5 - 9.3] | 6.4 [5.4 - 7.4] |
| Ar | 9.1 [5.4 - 12.9] | 8.5 [5.1 - 11.9] |
| Ca | 9.4 [3.4 - 15.7] | 9.0 [2.8 - 15.3] |
| Fe | 6.2 [4.6 - 7.9] | 6.9 [5.1 - 8.8] |
| Ni | 1 | 1 |
| $F_X^{(c)}$ (PN) | 1.45 (20.1) | 1.45 (28.2) |
| $F_X^{(c)}$ (MOS) | 1.56 (21.6) | 1.56 (30.4) |

All abundances are with respect to their solar values (Anders & Grevesse 1989). Brackets enclose 90% confidence intervals.

^a CSW model with decreased mass losses (0.5 of the nominal values), stellar wind velocities scaled by a factor of 1.5 (see text).

^b CSW model with increased binary separation (by a factor of 4), stellar wind velocities scaled by a factor of 1.5 (see text).

^c The observed X-ray flux (0.5 - 10 keV) followed in parentheses by the unabsorbed value. Units are $10^{-12} \text{ ergs cm}^{-2} \text{ s}^{-1}$.

of the both winds with the same factor has the advantage that the wind momentum ratio remains the same. This in turn facilitates the numerical hydrodynamic work needed prior to the spectral fits.

Finally, it is worth noting that the decreased mass losses and the increased binary separation both have similar effect, namely, they as well as the higher wind velocities make the NEI effects more pronounced (the Γ_{nei} values become smaller; see eq. [1]).

Figure 1 presents the results from the fits to the X-ray

spectrum of WR 147 for the cases discussed above. It is immediately seen that the CIE CSW models are not able to give acceptable fits ($\chi^2_\nu > 1.45$). On the other hand, the inclusion of NEI improves the quality of the spectral fits reaching acceptable values of $\chi^2_\nu = 1.10 - 1.15$, provided the wind velocities have values higher than the nominal ones by a factor of 1.4–1.6. Interestingly, if the Gorenstein (1975) conversion formula is used, the derived X-ray absorption from the best spectral fits is in a good correspondence with the data for the visual extinction deduced from other studies. This fact is also encouraging for the conclusion that the developments of the CSW model presented in this study are in the right direction. Examples of the most successful CSW models are shown in Fig. 2 and details about the fits are given in Table 1. It is seen from the figure that the theoretical models match very well the overall shape of the observed spectra with the exception of the soft energy part ($E < 0.8 \text{ keV}$). We believe that future data with higher photon statistics will help resolve this issue.

Thus, the results of the analysis of the X-ray emission from WR 147 show that there are at least three requirements for the numerical CSW model to be successful: (i) higher stellar wind velocities by a factor of 1.4 – 1.6; (ii) reduced mass losses for the stellar winds or larger binary separation (or both); (iii) the NEI effects must be taken into account. We note that the needed reduction factor for the mass loss of ~ 2 is well within the uncertainties for this parameter of the stellar winds in massive stars. But given the fact that the orbital parameters (e.g., inclination angle and eccentricity) are not well constrained for this binary system, much smaller corrections to the mass losses might be sufficient.

On the other hand, the wind velocities in massive stars are constrained much tighter usually on the basis of the P Cygni profiles of ultraviolet and optical spectral lines. This is not exactly the case of WR 147. Namely, Churchwell et al. (1992) derived a wind velocity of 900 km s^{-1} from the analysis of the HeI $2.058\mu\text{m}$ P Cygni line profile, and the spectral resolution was 500 km s^{-1} . Also from analysis of NIR observations with spectral resolution of 470 km s^{-1} (HeI $1.083\mu\text{m}$ emission line), Eenens & Williams (1994)

deduced 1100 km s^{-1} for the wind velocity in WR 147. Later, Hamann, Koesterke & Wessolowski (1995) proposed a 1000 km s^{-1} wind velocity, as their analysis was based on optical HeI lines. Based on *ISO-SWS* data with spectral resolution of $150\text{--}300 \text{ km s}^{-1}$, a wind velocity of 950 km s^{-1} was derived from the line profiles of the forbidden lines [NeIII] $15.5\mu\text{m}$, [SiIV] $10.5\mu\text{m}$, [CaIV] $3.21\mu\text{m}$ (van der Hucht et al. 1996; Morris et al. 2000). As we see, the wind velocity information on WR 147 comes mostly from IR spectra which not always had a very high spectral resolution. For a large sample of galactic WR stars Eenens & Williams (1994) compared the terminal wind velocities derived from infrared data (HeI $1.083\mu\text{m}$ and $2.058\mu\text{m}$ lines) with those from the conventional methods (based either on the P Cygni profiles of resonance lines in the ultraviolet region or on the widths of the optical lines). Interestingly, they have found that the values derived in IR are systematically lower by $\sim 30\%$.

If this is the case, then the wind velocity scaling factor derived here from the analysis of the X-ray data on the basis of the CSW model might not be unreasonable. Nevertheless, it is worth noting that if no solid evidence for higher stellar wind velocities are found in the future, this will pose serious problems for the CSW scenario as a central mechanism for the origin of X-rays in WR 147.

5 DISCUSSION

5.1 CSW Shocks: Collisional or Collisionless?

All the cases considered so far in this study assume a single-temperature hydrodynamic approximation, that is equal electron and ion temperatures. We recall that the thermal X-ray emission traces only the hot electrons, so, its analysis gives information mostly on the electron temperature in hot plasmas. If the plasma is heated through shocks, the kinetic energy of the gas flow is immediately (at the shock front) deposited to heavy particles (nucleons) and energy exchange between heavy and light particles (electron heating) occurs downstream via Coulomb collisions. Thus, some time is needed for the electron and ion temperatures to equilibrate. This timescale depends basically on the electron temperature and the nucleon number density (Braginskii 1958; Spitzer 1962), as it is longer in plasmas with higher temperature and lower density.

Although the electron heating mechanism at the shock front is not yet fully understood, it should be kept in mind that there are two general cases: electron heating in *collisional* and *collisionless* shocks. In the former case, the electrons initially attain a very low temperature mainly through adiabatic heating (Zeldovich & Raizer 1967). The situation could be very different in the latter case when various heating mechanisms might be at work and a range of degrees of temperature equilibration is possible up to equal electron and ion temperatures (e.g., McKee 1974; Papadopoulos 1988; Cargill & Papadopoulos 1988). These possibilities are usually described by a simple parameter that relates the electron temperature at the shock front to the postshock mean plasma temperature, $\beta = T_e/T$ (thus $\beta \approx 0. - 1.$).

As the effects of unequal electron and ion temperatures are important in high temperature, rarefied plasmas, they are thus expected to play a role for colliding stellar

winds in wide binaries. Such models were first considered by Zhekov & Skinner (2000) who also introduced a dimensionless parameter that determines the relative importance of electron heating via Coulomb collisions downstream in the interaction region (see eq.[1] in their work). For the nominal wind and binary parameters of WR 147 (§ 3.4), the value of this dimensionless quantity suggests that the temperature equilibration effects can be neglected when modelling the X-rays from this object.

On the other hand, as was shown in § 4 the successful CSW models require higher wind velocities, and reduced mass loss or larger binary separation than the nominal values of these parameters. This in turn means a slower temperature equilibration, that is a higher chance for the unequal electron and ion temperatures to affect the X-ray emission from WR 147. To explore this possibility, we ran models (both NEI and CIE) with $\beta = 0.2$, and the main result is the lower quality of the spectral fits (see Fig. 1). Obviously, the reason for this is that the temperature equalization timescale is relatively long, therefore, the electron temperature remains below the mean plasma temperature in the interaction region. Guided by this and the fact that models with CIE plasma cannot reproduce the X-ray spectrum well, more CSW models with different values of β were considered as preference was given to cases with velocity scaling factor larger than 1.5. Some results from the spectral fits with these NEI models are shown in Fig. 3. It is seen that acceptable fits ($\chi^2_\nu = 1.10 - 1.15$) are possible if the wind velocities are of $1.5 - 2.0$ times larger than their nominal values, and for a high degree of the temperature equilibration ($\beta \geq 0.4$). The best fits for high velocity scaling factors are obtained with a lower initial electron temperature relative to the mean postshock gas temperature.

It is then interesting to check whether good spectral fits are possible also for very low values of the initial electron temperature. To do so we ran NEI CSW models with $\beta = 0.001$, a value that could be considered typical for collisional shocks. The results are shown in Fig. 4 and it is seen that no acceptable fits are possible for the ‘reasonable’ values of the velocity scaling factor.

Therefore, it is conclusive that the CSW shocks in WR 147 are *collisionless!*

5.2 CSW Models vs. Discrete Temperature Models

The analysis presented here has shown that the CSW model can explain the *XMM-Newton* X-ray data for WR 147, provided that some reasonable adjustments to the currently accepted mass-loss parameters and orbital separation are made. On the other hand, it was shown in S07 that much simpler models, discrete temperature ones, could be equally successful, as the quality of the spectral fits shows. The obvious advantage of the CSW model is that it describes a real physical situation which is likely present in massive binaries, but what could we learn from the application of these simpler models?

It is worth recalling that the interaction region in CSW binaries is temperature stratified, thus, its X-ray emission is a sum of individual contributions from plasmas with a range of temperatures weighted by their emission measure. It is then not surprising that in such a case the total (‘in-

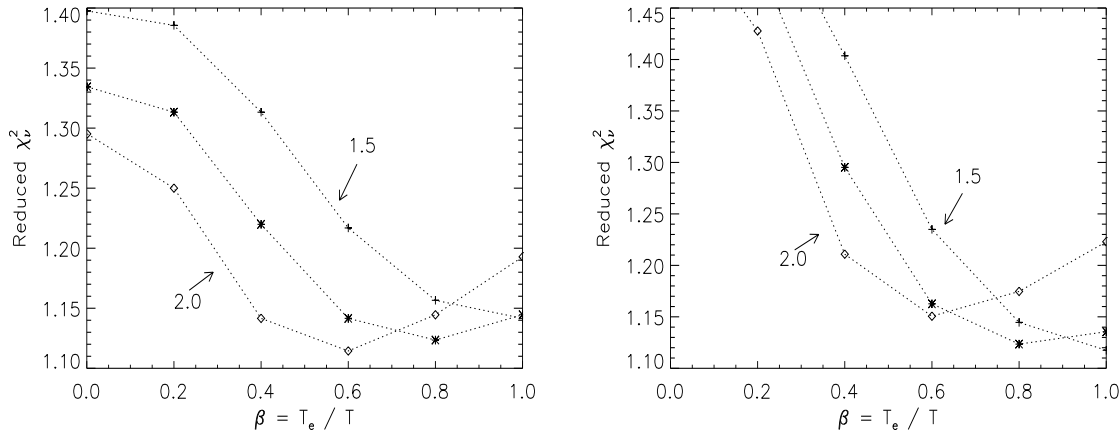


Figure 3. Quality of the fit for NEI CSW models ($\eta = 0.028$) with different degrees of initial temperature equilibration ($\beta = T_e/T$). Shown are cases with wind velocity increased by a factor of 1.5, 1.7, and 2.0, respectively. **Left panel:** Mass-loss rates scaled while the binary separation is kept at its ‘nominal’ value. **Right panel:** The binary separation is scaled while mass-loss rates have their ‘standard’ values. The degrees of freedom in all the fits are $\nu = 332$.

tegrated’) X-ray spectrum can be quite well represented by isothermal plasma emission with some ‘average’ temperature, and its value must be lower than the maximum plasma temperature in the shocked plasma. We note that the successful NEI CSW models require a wind velocity scaling factor of at least ~ 1.4 (see § 4). Given the nominal wind parameters (§ 3.4), this suggests for the shocked WR wind a maximum plasma temperature of ~ 4 keV, which is found near the line of centers in CSW binaries (for a strong shock with adiabatic index $\gamma = 5/3$ the postshock temperature is $kT = 1.956\mu v_{1000}^2$, keV, where v_{1000} is the shock velocity in units of 1000 km s^{-1}). From such a point of view it is understandable why a constant temperature plane-parallel shock model with $kT \simeq 2.7$ keV does a good job (S07). This model (*vpshock* in XSPEC) has the most important characteristic of the CSW models for WR 147, namely, it takes into account the NEI effects. As also discussed in S07, the fact that the temperature of this shock model was higher than the maximum expected for the currently accepted WR wind velocity (950 km s^{-1}) was already indicative that higher stellar wind velocities might be present in this object. These authors reached similar conclusions on the basis of their discrete two-temperature models with CIE.

Thus, the use of simpler models for representing the X-ray emission from hot plasmas can, on the one hand, be very helpful by guiding further modelling that elaborates a real physical picture in the studied objects. On the other hand, it may also pose some problems for interpreting the results when models bearing quite different physics (e.g. CIE vs. NEI) are equally successful, as is the case for WR 147. A solid argument in favour of the NEI case here could be that the more elaborated models are successful only if these effects are taken into account. But, it will be much more valuable if a purely observational evidence is found that helps resolve this issue. For example, future gratings data with good photon statistics will detect relatively strong forbidden lines in the He-like triplets of various elements if the NEI effects play an important role. Such observational data

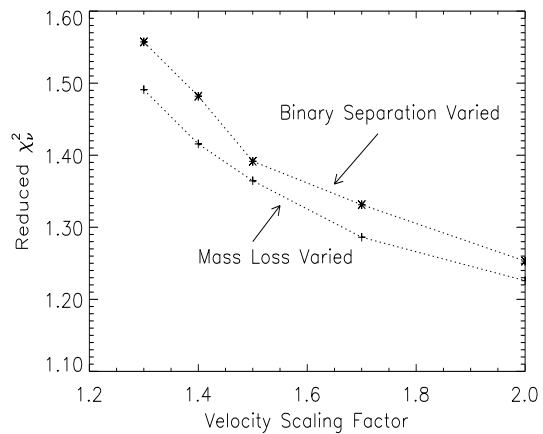


Figure 4. Quality of the fit for NEI CSW models ($\eta = 0.028$) with a very low degree of initial temperature equilibration, typical for collisional shocks ($\beta = 0.001$). The degrees of freedom in all the fits are $\nu = 332$.

will thus reveal where exactly the X-ray emission forms, i.e. in the rarified hot plasma of the CSW interaction region.

5.3 CSW Models and Nonthermal Emission from WR 147

We recall that wide CSW binaries are not only sources of strong X-ray emission but are non-thermal radio emitters as well, and WR 147 is no exception to the rule. Relativistic electrons must be available in such objects, thus, the strong shocks that shape the CSW zone in these systems are likely places where the electrons are being accelerated. Pittard et al. (2006) have presented this idea in a quantitative manner developing a numerical model of the synchrotron radio emission from CSW binaries. Although this model is not self-consistent it was the first attempt to consider the non-thermal radio emission from such objects

in detail. Naturally, their theoretical predictions were then confronted with the detailed radio observations of WR 147. One of the main conclusions from this analysis was that the acceleration of relativistic electrons appear to be very efficient requiring up to half of the thermal energy of the postshock plasma to be deposited into non-thermal particles. We must note that if this were the case, one of the basic consequences for the CSW zone would be a noticeable decrease of the temperature of the shocked hot gas.

Contrary to this, our analysis of the *XMM-Newton* data for WR 147 has shown that the X-ray emitting plasma is hotter than suggested by the nominal parameters of the stellar winds in this object. It is then conclusive that there is evidence that the CSW model is capable of explaining the X-ray emission in the wide WR+OB binary WR 147 but further refinements are needed to successfully describe the corresponding non-thermal radio emission from this object.

6 CONCLUSIONS

We developed an improved colliding stellar wind model that includes the effects of nonequilibrium ionization in hot plasmas, and the *XMM-Newton* X-ray spectra of WR 147 were analyzed in the framework of this model. The basic conclusions are the following.

1. If the ‘standard’ (§ 3.4) stellar wind parameters and binary separation are assumed, the CSW model predicts an emission measure of the hot plasma that is 3 – 4 times larger than what is needed to explain X-ray emission from WR 147. Also, the shape of the theoretical spectrum does not match well that of the observed spectra, especially, at higher energies ($E \geq 4$ keV). It is then concluded that hotter plasma must be present in the CSW zone of this object, and as proposed by S07, such a hotter plasma could be the result of higher wind velocities.

2. By exploring a range of stellar wind velocities, it is shown that CSW models with nonequilibrium ionization are able to satisfactorily fit the observed X-ray spectra of WR 147, provided the stellar winds are faster by a factor of 1.4 – 1.6. To resolve the issue of the increased emission measure, the mass loss rate should be decreased by a factor ~ 2 or the binary separation must be increased by a factor ~ 4 compared to the nominal values of these parameters. All these parameter changes are within their corresponding uncertainties. It is worth emphasizing that in the framework of the CSW picture only NEI models can correctly represent the observed X-ray data from this object.

3. Different electron and ion temperatures are usually found in shock heated rarefied plasmas, which is likely the case in wide CSW binaries. Models that assume various degrees of temperature equalization in the CSW shocks were confronted with the X-ray data of WR 147. Only NEI models with very high temperature equalization were successful, a case typical for collisionless shocks. On the other hand, models that assume a very low electron postshock temperature, which is characteristic of collisional shocks, cannot explain the observed data. Therefore, the analysis of the X-ray spectra of WR 147 finds evidence that the CSW shocks in this object must be *collisionless*.

4. If future X-ray grating observations of WR 147 with good photon statistics are obtained, they are expected to

reveal strong forbidden lines in the He-like triplets of various elements. The detection of strong f lines would be the most solid argument that the hot plasma in WR 147 is in a state of nonequilibrium ionization. It will then be evident that the X-ray emission in WR 147 originates in rarefied plasma that is characteristic of CSWs in wide binary systems.

7 ACKNOWLEDGMENTS

The author would like to thank Steve Skinner for the careful reading of the manuscript and for his helpful comments. This work is based on observations with *XMM-Newton*, an ESA science mission with instruments and contributions directly funded by ESA states and USA (NASA). Also, the author appreciates the helpful comments by an anonymous referee.

REFERENCES

- Abbott D.C., Biegging J.H., Churchwell E., Torres A.V., 1986, ApJ, 303, 239
- Arnaud K. A. 1996, in Jacoby G., Barnes J., eds., ASP Conf. Ser. Vol. 101, Astronomical Data Analysis Software and Systems, Astron. Soc. Pac. San Francisco, p.17
- Anders E., Grevesse N., 1989, Geochimica et Cosmochimica Acta, 53, 197
- Borkowski K.J., Lyerly W.J., Reynolds S.P., 2001, ApJ, 548, 820
- Braginskii S.I., 1958, Soviet Phys-JETP, 6, 358
- Caillault, J.-P., Chanan, G. A., Helfand, D. J., Patterson, J., Nousek, J. A., Takalo, L. O., Bothun, G. D., Becker, R. H., Nature, 313, 376
- Cargill P.J., Papadopoulos K., 1988, ApJ, 329, L29
- Churchwell E., Biegging J.H., van der Hucht K.A., Williams P.M., Spoelstra T.A.Th., Abbott D.C., 1992, ApJ, 393, 329
- Contreras M.E., Montes G., Wilkin F.P., 2004, Rev. Mex. Astron. Astrofis., 40, 53
- Contreras M.E., Rodriguez L.F., 1999, ApJ, 515, 762
- Contreras M.E., Rodriguez L.F., Gomez Y., Velazquez A., 1996, ApJ, 469, 329
- Dougherty S.M., Pittard J.M., Kasian L., Coker R.F., Williams P.M., Lloyd H.M., 2003, A&A, 409, 217
- Eenens P.R.J. & Williams P.M., 1994, MNRAS, 269, 1082
- Hamann W.-R., Koesterke L., Wessolowski U., 1995, A&A, 299, 151 -
- Hughes J.P., Helfand D.J., 1985, ApJ, 291, 544
- Liedahl D.A., 1999, in X-ray Spectroscopy in Astrophysics, eds. J. van Paradijs and J.A.M. Bleeker, LNP 520, 189
- McKee C.F., 1974, ApJ, 188, 335
- Mewe R., 1997, in X-ray Spectroscopy in Astrophysics, eds. J. van Paradijs and J.A.M. Bleeker, LNP 520, 109
- Moran J.P., Davis R.J., Spencer R.E., Bode M.F., Taylor A. R., 1989, Nature, 340, 449
- Morris P.M., van der Hucht K.A., Crowther P.A., Hillier D.J., Dessart L., Williams P.M., Willis A.J., 2000, A&A, 353, 624
- Myasnikov A.V., Zhekov S.A., 1993, MNRAS, 260, 221 (MZh93)
- Niemela V.S., Shara M.M., Wallace D.J., Zurek D.R., Mofat A.F.J., 1998, AJ, 115, 2047

- Papadopoulos K., 1988, *Ap&SS*, 144, 535
- Pittard J.M., Stevens I.R., Williams P.M., et al. 2002, *A&A*, 388, 335
- Pittard J.M., Dougherty S.M., Coker R.F., O'Connor E.O., Bolingbroke N.J., 2006, *A&A*, 446, 1001
- Setia Gunawan D.Y.A., de Bruyn A.G., van der Hucht K.A., Williams P.M., 2001, *A&A*, 368, 484
- Skinner S.L., Itoh M., Nagase F., Zhekov S.A., 1999, *ApJ*, 524, 394 (S99)
- Skinner S.L., Zhekov S.A., Güdel M., Schmutz W., 2007, *MNRAS*, 378, 1491 (S07)
- Spitzer L., 1962, *Physics of Fully Ionized Gases* (New York: Interscience)
- van der Hucht K.A., Cassinelli J.P., Williams P.M., 1986, *A&A*, 168, 111
- van der Hucht K. A., Morris P. W., Williams P. M., et al., 1996, *A&A*, 315, L193
- Williams P.M., Dougherty S.M., Davis R.J., van der Hucht K.A., Bode M.F., Setia Gunawan D.Y.A., 1997, *MNRAS*, 289, 10
- Zeldovich Ya.B., Raizer Yu.P., 1967, *Physics of Shock Waves and High-Temperature Hydrodynamic Phenomena* (New York: Academic)
- Zhekov S.A., Skinner, S.L. 2000, *ApJ*, 538, 808